



Hardware-in-the-Loop Implementation of the Hybrid FPA-P&O Approach for Optimizing Photovoltaic Systems under Partial Shading Conditions

Fares Bettahar ^{a,*}, Sabrina Abdeddaim ^a, Achour Betka ^a

^a *Electrical Engineering Department, Faculty of Sciences and Technology, University of Biskra, Algeria*

ARTICLE INFO

Article history:

Received September 27, 2024

Accepted June 22, 2025

Available online June 24, 2025

Published June 26, 2025

Keywords:

Photovoltaic generation systems,

MPPT,

FPA-P&O,

PSCs,

Hardware-in-loop.

ABSTRACT

Efficient solar panel power generation is crucial for sustainable energy systems, particularly as PV systems are often installed near urban areas where shadows from buildings and trees can cause fluctuations in power output. Hence, it is essential to employ Maximum Power Point Tracking (MPPT) to consistently ascertain the MPP of the PV module in real-time, irrespective of the weather conditions. The present paper aims to propose a hybrid Maximum Power Point Tracking (MPPT) technique that uses the Flower Pollination Algorithm (FPA) and Perturb and Observe (P&O) methods, applied to photovoltaic systems under partial shading conditions PSCs. The photovoltaic system was implemented using a Hardware-in-loop (HIL) setup. The proposed MPPT technique is compared with the classical P&O and standard FPA. In addition, the proposed algorithm gives 99 % tracking efficiency under various shading patterns. The efficacy of the proposed algorithm is overall superior compared to other methods in terms of statistical analysis and tracking time and almost zero oscillation near GMPP. These results underscore the significant potential of the P&O-FPA algorithm to enhance photovoltaic performance, particularly in situations where partial shading conditions.

1. INTRODUCTION

The increasing energy demands across industries and sectors have created a pressing need for electrical energy (Krishna & Kumar, 2015). However, the reliance on fossil fuels like oil and coal is contributing to global warming and environmental degradation (Bollipo et al. 2020). As a result, there is a growing demand for sustainable and renewable energy sources. Photovoltaic (PV) energy, derived from solar

* Corresponding author, E-mail address: fares.bettahar@univ-biskra.dz

Tel : + 213 74507889



power, offers a promising solution. It is a clean and abundant renewable energy resource suitable for residential, industrial, and commercial applications (Yang and Wen 2018).

Photovoltaic (PV) cells are at the forefront of renewable energy technology, possessing a unique ability to directly convert light energy from the sun into electrical energy (Bhukya and Kota 2018). However, an inherent challenge in solar energy utilization lies in the potential obstruction of sunlight, which can impede the efficient harnessing of the received solar energy. This obstruction can manifest as shadows, clouds, buildings, or tree leaves that cast shadows on the PV cell surface. When sunlight is partially blocked, multiple peak power points may occur within the nonlinear current-voltage (I-V) and power-voltage (P-V) characteristics of the PV cell (Mai et al. 2024). These peak power points include the global maximum power point (GMPP) and local maximum power points (LMPP). Attaining and maintaining the GMPP, especially in the presence of numerous LMPPs, is essential to ensure optimal energy conversion from the PV module. To address this challenge, the implementation of a technology Maximum Power Point Tracking (MPPT) becomes necessary.

The literature presents a wide array of Maximum Power Point Tracking (MPPT) methods, as in Baba et al. (2020) which provide detailed coverage of all types. These types were classified based on criteria like tracking speed efficiency, Cost, and Complexity. Perturb and Observe (P&O) and Incremental Conductance (INC) of the easiest and most widely used techniques. However, (Chellal et al. 2021) these methods fail to effectively track the MPP under varying irradiation conditions. Conversely, AI methods for MPPT show impressive tracking capabilities and fast speeds. Nevertheless, it is crucial to mention that these strategies frequently require intricate control circuitry and thorough data processing for system training beforehand.

In recent years, there has been a notable surge in the utilization of metaheuristic optimization techniques (Nassef et al. 2023). These approaches offer a promising avenue to address the limitations inherent in conventional methods and artificial intelligence (AI) based Maximum Power Point Tracking (MPPT) techniques. Metaheuristic algorithms distinguish themselves through their ability to optimize globally, ensuring the accurate identification of the Global Maximum Power Point (GMPP) within the operational range of a photovoltaic (PV) system. Among the plethora of metaheuristic optimization methods, Particle Swarm Optimization (PSO), Artificial Bee Colony (ABC), Cuckoo Search (CS), Flower Pollination Algorithm (FPA), Grey Wolf Optimization (GWO), Genetic Algorithm (GA), Bat Algorithm (BA), and Horse Herd Optimization (HAO), among others, stand out. These algorithms exhibit robust stability and adapt to fluctuating environmental conditions and system parameters. However, despite these advantages, they may be very slow to explore the global point.

Recent innovative research has emerged, showcasing hybrid techniques that amalgamate the speed of traditional approaches with the precision and efficacy of metaheuristic methods. In this regard, a hybrid technique that integrates Perturb and Observes (P&O) with the Flower Pollination Algorithm (FPA) has been introduced with details of how a direct control FPA-P&O is used to track the GMPP for a photovoltaic(PV)system, where FPA operates during the initial stages for tracking of the GMPP and P&O algorithm during the final stages to achieve faster convergence towards the GMPP. The FPA-P&O algorithm was implemented and tested alongside classical P&O and standard FPA algorithms using real-time Hardware-In-the-Loop (HIL) with two dSPACE 1104 Controller Boxes, known for their high accuracy and real-time performance. This HIL approach is validated by previous research (Fares et al., 2023). The results show that FPA-P&O has a greater advantage in tracking accuracy compared with other methods and achieves convergence quicker than GMPP. This essay is structured as follows: The modelling of the photovoltaic system, which involves both the PV panel and the DC-DC converter, is presented in Section 2. The proposed approach is then described in Section 3. Sections 4 and 5 provide and explain, respectively, the HIL results. A conclusion brings this paper to its conclusion.

2. DESCRIPTION AND MATHEMATIC MODEL OF PV SOLAR SYSTEM

2.1 PV System Modelling

A photovoltaic cell functions as a perfect current source, producing a current correlated to the amount of light it receives, alongside a diode representing the cell's p-n junction area. Figure 1 displays a representation of a junction connected to a load and illuminated by photovoltaic energy. It can be simplified as a current generator in parallel with a single diode and in series with a resistance R_s , with the assumption that the parallel resistance can be ignored (Fares et al. 2023). The relationship between the current and voltage in PV model can be written as (Samano-Ortega et al. 2020):

$$I_{pv} = I_{ph} - I_d \quad (1)$$

$$I_{pv} = \frac{G}{G_r} (I_{sc} + K_i(T - T_r)) - I_{sc} - I_{op} * \left[\exp \left(\frac{-(V_{op} + R_s * I_{op})}{V_{th}} \right) \right] \quad (2)$$

Where: T is the temperature in Kelvin (K), T_r is the reference temperature of the cell in Kelvin (K) ($=25^\circ\text{C} + 273$), G is the solar radiation in watt/square meter (W/m^2), G_r is the reference insolation of the cell ($=1000 \text{ W}/\text{m}^2$) and V_{th} is the thermal voltage of the module.

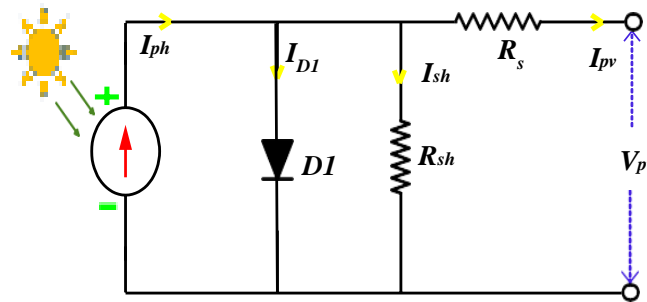


Fig 1. Equivalent circuit of solar PV module.

In this paper, the solar panel Monocrystalline (Sharp) NTR5E3E/NT175E1 is considered. The specifications of this solar panel at steady state conditions (STC) of 25°C and $1000 \text{ W}/\text{m}^2$ are the parameters used in the simulations listed in (Fares et al. 2025, Table 1).

2.2 Partial Shading of PV System

Large-scale deployment of solar panels for electricity generation inherently increases the likelihood of encountering partial shading conditions. Such shading can arise from various environmental and structural factors, including intermittent cloud cover, surrounding buildings, vegetation, and airborne particulates such as dust or sand during storms (Fekkek et al. 2019). Partial shading significantly affects the performance of photovoltaic (PV) systems by creating non-uniform irradiance levels across different sections of the solar array. This mismatch leads to multiple peaks in the power-voltage (P-V) and current-voltage (I-V) curves, manifesting as both global maximum power points (GMPP) and local maximum power points (LMPP). As a result, the overall energy output of the system may suffer substantial reductions, with power losses ranging from 10% up to 70% depending on the severity and pattern of the shading (Chauhan et al. 2019).

To systematically investigate the impact of shading and evaluate the tracking efficiency of different MPPT strategies, the study employed two distinct PV array configurations. The first configuration consisted of four PV modules connected in series (4S), while the second utilized a combination of two PV modules connected in series, with two such series strings connected in parallel (2S2P). These configurations were specifically designed to emulate common partial shading scenarios and to facilitate comparative analysis. The physical arrangement and the resulting shading patterns for each setup are depicted in Figures 2 and 3, respectively, providing a controlled basis for analyzing system behavior under different irradiance distributions.

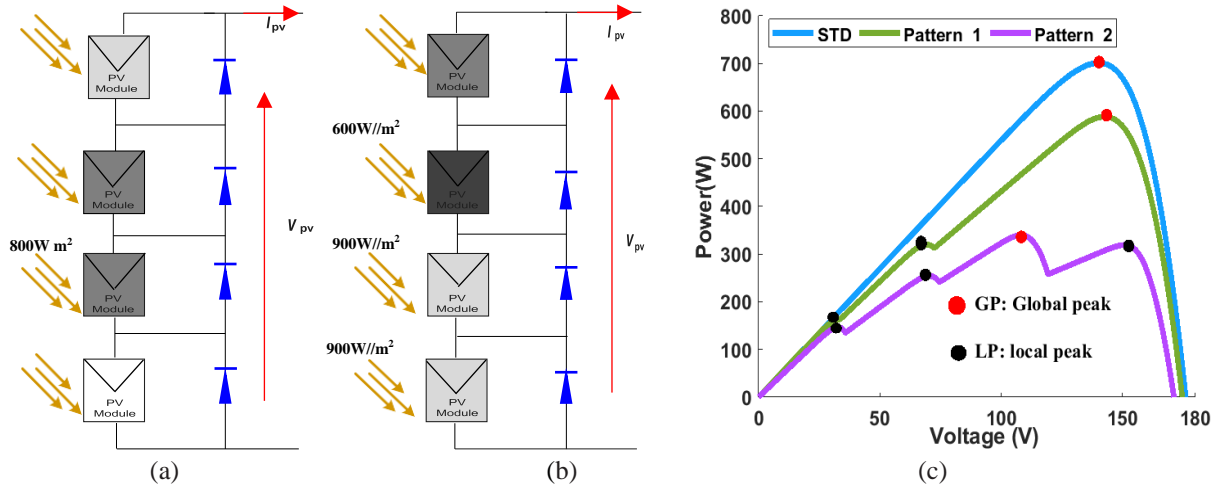


Fig 2. 4S set-up in various shading scenarios. (a) Shade Pattern 1. (b) Shade pattern 2. (c) P –V curve

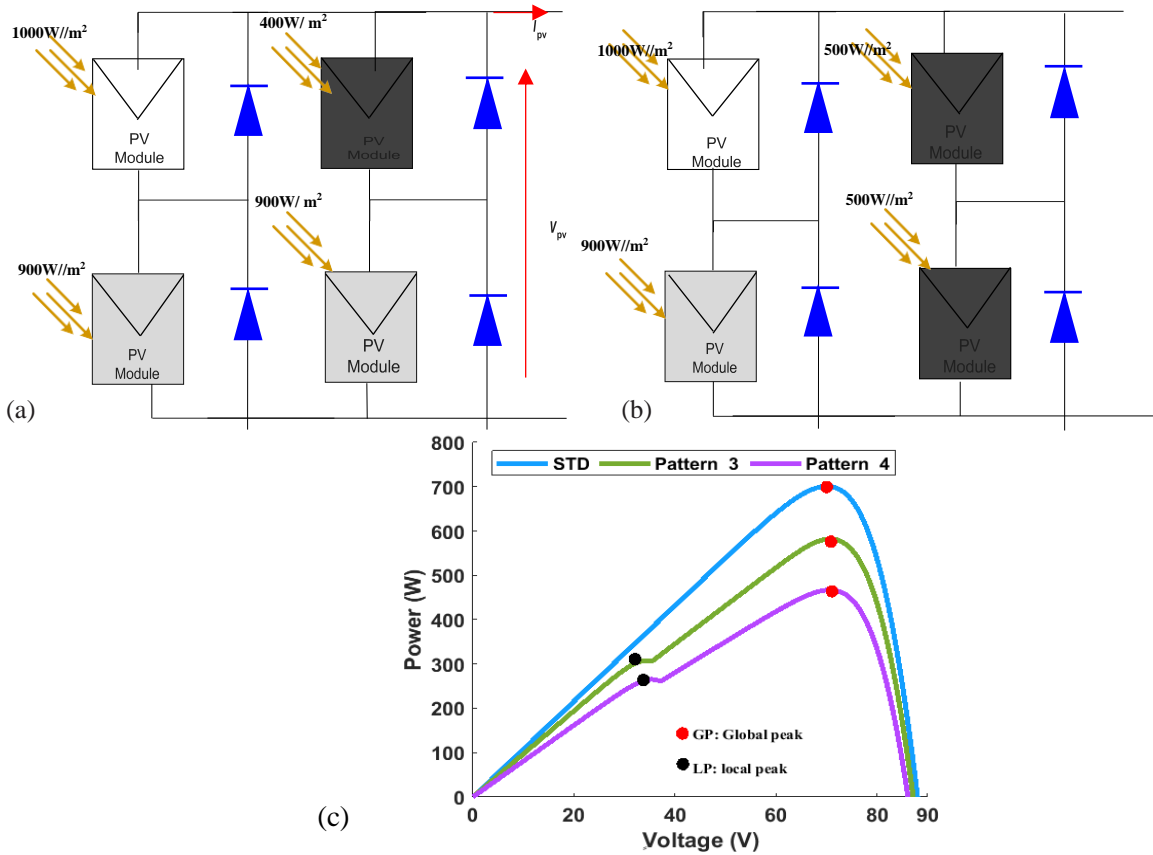


Fig 3. 4S set-up in various shading scenarios. (a) Shade Pattern 1, (b) Shade pattern 2, (c) P –V curve

2.3 DC/DC Converter

The use of a power converter interface between the solar panel and the load is essential to ensure maximum power transfer and efficiency (Zhao et al. 2019). A boost converter was used to address the issue of the PV module output power not being maximized when directly connected to the load (Fekkak et al. 2019). Figure 4 shows a block diagram with a PV system, MPPT controller, and boost converter. The boost converter is composed of several components, including an input capacitor C1, inductor L, resistor, diode, MOSFET (S), and output capacitor C2. The control algorithm measures the input voltage and current and adjusts the duty cycle D accordingly to track the maximum power point. This involves continuously varying the duty cycle to find the point where the input power is maximized. Subsequently, the PWM controller will direct the generation of suitable switching signals for switch S in the boost converter. When switch S is activated, diode D is reverse-biased, and input voltage V_{pv} is connected to inductor L. Turning off the switch S in the boost converter results in a reversal of polarity across the inductor, leading to a higher voltage across diode D compared to input voltage V_{pv} . In the context, the relationship between the input voltage (V_{pv}) and the output voltage (V_0) is given as:

$$V_0 = \frac{V_{pv}}{1 - D} \quad (3)$$

The characteristics of the DC-DC boost converter are detailed in (Bettahar et al. 2023).

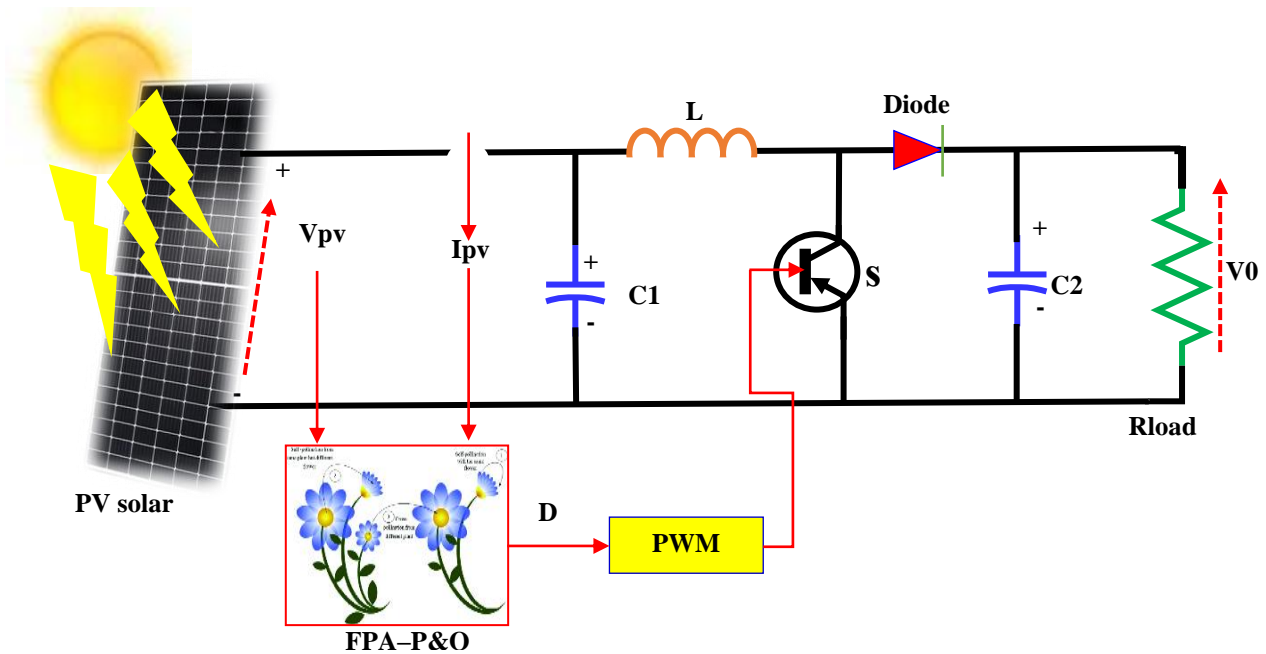


Fig 4. The electrical circuit of a Boost converter combined with a PV system structure with MPPT control

3. PROPOSED FPA and P&O MPPT ALGORITHM

The Flower Pollination Algorithm (FPA) is an optimization algorithm that mimics the process of pollination in flowers (Mohanty et al. 2017). It uses global and local pollination operations to generate new candidate solutions. Global pollination involves transferring the best solution to other flowers in the population, while local pollination modifies a solution by adding or subtracting a random value. The equations for global and local pollination are given by Eq. (4) and Eq. (7) (Senapati et al. 2023). The algorithm aims to optimize a given objective function by iteratively updating the solutions based on

global and local pollination operations. The process continues until convergence towards the optimal solution is achieved.

- Local Pollination

Local pollination involves adjusting a solution by adding or subtracting a random value. The equation for local pollination is:

$$x_{i,k+1} = x_{i,k} + \epsilon(x_{j,k} - x_{f,k}) \quad (4)$$

Where $x_{j,k}$ and $x_{f,k}$ are randomly chosen pollen from different flowers of the same type and ϵ is a random value ranging between 0 and 1.

- Global Pollination

Global pollination entails transferring the Global best solution (gbest) to other flowers within the population. The equation for global pollination is:

$$x_{i,k+1} = x_{i,k} + \gamma L(\lambda)(gbest - x_{i,k}) \quad (5)$$

where: $x_{i,k}$ represents the solution of the i th flower in the k th iteration. $\gamma L(\lambda)$ denotes the Levy flight displacement, as defined in Eq. (6).

- Levy Flight Displacement

The Levy flight displacement is expressed as:

$$L(\lambda) \approx \frac{\lambda \cdot \Gamma(\lambda) \cdot \sin\left(\frac{\pi\lambda}{2}\right)}{\pi \cdot S^{(1+\lambda)}} \quad (6)$$

Where λ is typically set to 1.5, $\Gamma(\lambda)$ denotes the standard gamma function and S is defined by $S = \mu / (|v|^{1/\lambda})$

Where μ and v obey normal distribution, $\mu \sim N(0, \sigma^2)$ and $v \sim N(0,1)$.

$$\sigma^2 = \left[\frac{\Gamma(1+\lambda)}{\lambda \Gamma((1+\lambda)/2)} \cdot \frac{\sin(\lambda\pi/2)}{2^{(\lambda-1)/2}} \right]^{-1/\lambda} \quad (7)$$

The P&O MPPT method adjusts the operating point, observes power changes before and after, and adapts the duty cycle according to a defined rule [19] to track the MPP.

$$\begin{aligned} D_{\text{new}} &= D_{\text{old}} + \phi \quad \left(\text{if } P > P_{\text{old}} \right) \\ D_{\text{new}} &= D_{\text{old}} - \phi \quad \left(\text{if } P < P_{\text{old}} \right) \end{aligned} \quad (8)$$

The hybrid MPPT algorithm starts with FPA to find the Global Peak (GMMP) and then switches to P&O. P&O MPPT begins at the best flower location from FPA when the flowers converge.

On the other hand, boosting the quantity of flowers improves MPP precision while also increasing computational requirements. Hence, maintaining a moderate amount of flowers, in this study used four, is believed to achieve a balance between MPP precision and computational speed. The following steps are adopted to implement the hybrid MPPT algorithm:

1. Initialization: Initialize the duty cycle randomly and store it in a matrix $D = [D1, D2, D3, D4]$. D is limited between 0 and 1.
2. Maximizing PV Output Power: Activate the converter to maximize the PV array output power ($P_{pv} = V_{pv}I_{pv}$).
3. Duty Cycle Adjustment: Adjust the duty cycle based on the FPA equation Eq. (5).

$$D_i^{k+1} = D_i^k + \gamma L(\lambda) (g_{\text{best}} - D_i^k) \quad (9)$$

4. Convergence: Repeat the duty cycle adjustment process until all solutions converge towards the MPP.
5. Tracking GMPP: After locating the MPP, initiate the P&O loop for tracking the maximum power GMPP. Choose a small step size (ϕ) to reduce oscillations in PV output power and improve tracking efficiency.

4. RESULTS AND VALIDATION USING HIL SETUP

To assess the practicality and effectiveness of the proposed FPA-P&O MPPT algorithm, we employed a Hardware-in-the-Loop (HIL) approach that integrates dSPACE ds-1104 (1) and dSPACE ds-1104 (2), as depicted in Figure 5. In the dSPACE ds-1104 (2) environment, simulated the PV array, DC/DC boost converter and Rload, while the implementation of the MPPT algorithms took place in the dSPACE ds-1104 (1) environment. The HIL results were obtained based on the settings listed in Tables 1,2 and parameters of FPA algorithm $D1=0.1$, $D2=0.3$, $D3=0.6$, $D4=0.9$ with step size of P&O $\phi=0.005$ in all Cases. To efficiently manage the real-time dynamics of the power system, we configured the solver in MATLAB with a fixed time step of $1e-4$ s, ensuring high time resolution. especially when dealing with rapidly changing irradiance levels caused by moving shadows.

It also addresses the limitation of the dSPACE ds-1104, where the time step is restricted to equal or less than $1e-4$ s and we increased the signal duty cycle by a factor of 15.

The control system utilizes two ADC channels to capture both I_{pv} and V_{pv} obtained from the power system. Furthermore, a solitary duty cycle is transmitted through a single DAC (Digital-to-Analog Converter) channel. On the other hand, the power system's DAC channels transmit a lone value of I_{pv} and V_{pv} . Simultaneously, a duty cycle is captured from the control system using an ADC channel.

The maximum power output for Perturb and Observe (P&O), Flower Pollination Algorithm (FPA) and the hybrid FPA-P&O under four shading patterns was assessed. In pattern 1, as shown in Fig. 2(a), four PV modules were exposed to irradiances of 900, 800, 800, and 1000 W/m². This case produced one global peak (GMPP = 588.8 W) and two local peaks (LMPP1 = 180.7 W and LMPP2 = 310 W), as depicted in the P-V curve in Fig. 2(c). The hybrid method achieved a GMPP of 588.7 W after a convergence time of 0.25 s, while FPA took 0.76 s to reach a GMPP of 572.02 W. On the other hand, P&O was misled by the second local peak (LMPP2 = 310 W) and exhibited large oscillations around this point, as shown in Figure 6(a).

Pattern 4 is shown in Fig. 3(b). PV modules were exposed to 1000, 800, 500, and 500 W/m² irradiance, resulting in one LMPP at 286.5 W and one GMPP at 467.1 W, as shown in Fig. 3(c). The P&O method achieved 460.2 W with significant steady-state oscillations, FPA attained 465 W in 0.89 seconds, and the hybrid algorithm briefly reached 467.08 W in 0.27 seconds, as shown in Fig. 7(b).

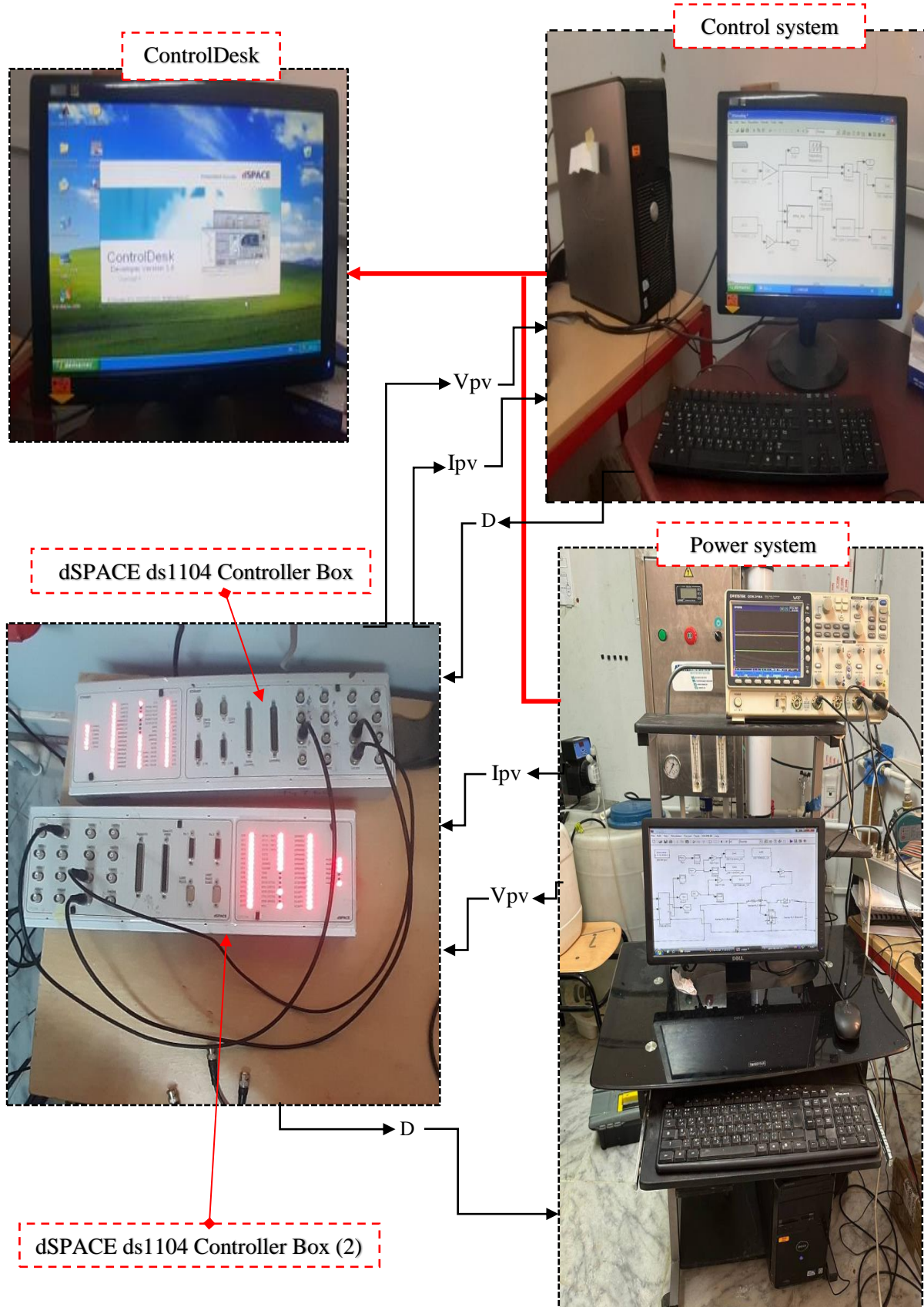


Fig 5. Hardware in the loop setup.

Pattern 2 represents severe shading due to the significant differences in received solar irradiation, as shown in Fig. 2(a). Four PV modules were exposed to irradiances of 700, 600, 800, and 700 W/m², resulting in a GMPP of 339.9 W. The P-V curve, accompanied by three local peaks (LMPP1 = 186 W, LMPP2 = 260.34 W, and LMPP3 = 325.2 W), is shown in Fig. 2(b) and Fig. 2(c). In 0.28 seconds, the hybrid method achieved a GMPP of 339.8 W, with no steady-state oscillations. The FPA method obtained a GMPP of 330 W after 0.78 seconds. In contrast, the P&O method reached MPP2 at 260.34 W, exhibiting minor steady-state oscillations, as depicted in Figure 6(b).

The HIL experiment dynamic responses of the PV array power in Figures 6c and 6d correspond to Pattern 1 and Pattern 2, respectively, which is in good agreement with the simulation findings displayed in Figure 6a and 6b. This result validates the proper functioning of the hybrid-based MPPT algorithms.

Figures 7(a) and 7(b) present the PV power achieved with MPPT using Patterns 3 and 4, respectively.

Pattern 3 is shown in Fig. 3(a). PV modules were exposed to 1000, 900, 400, and 900 W/m² irradiance, demonstrating a P-V curve in Fig. 3(c) with a GMPP at 582.2 W and an LMPP at 307 W. The hybrid approach swiftly attained a GMPP of 582.1 W within 0.29 s, effectively avoiding steady-state oscillations. Conversely, the FPA method required 0.89 seconds to reach and stabilize at 570.5 W, while the P&O method reached 581 W but experienced significant steady-state oscillations, as shown in Figure 7(a).

The dynamic responses of the PV array power in Figures 7(c) and 7(d) from the HIL experiment correspond to Pattern 3 and Pattern 4, respectively. These results align closely with the simulation findings shown in Figures 7(a) and 7(b), validating the effective performance of the hybrid-based MPPT algorithms.

5. COMPARING THE PERFORMANCES OF P&O, FPA AND HYBRID

The results of this work confirm that the hybrid method is fast and efficient compared to individual methods for the MPPT optimization problem. This section offers a mathematical demonstration that the hybrid approach ensures discovering the top global optimal solution for the optimization-based MPPT, resulting in the global maximum power point GMPP. Statistical analysis was utilized to assess the effectiveness of the suggested MPPT techniques by examining their sensitivity and robustness to different instances of partial shading. The relative error (RE), mean absolute error (MAE), and root mean square error (RMSE) are defined by:

$$\text{RE error} = \frac{\sum_{i=1}^n (P_{pvi} - P_{pv})}{P_{pv}} * 100\% \quad (10)$$

$$\text{RME error} = \frac{\sum_{i=1}^n (P_{pvi} - P_{pv})}{n} \quad (11)$$

$$\text{RMSE error} = \sqrt{\frac{\sum_{i=1}^n (P_{pvi} - P_{pv})^2}{n}} \quad (12)$$

where P_{pvi} is power at the maximum point, P_{pv} is the maximum power tracked and n represents the number of samples. These values are determined using 400000 samples.

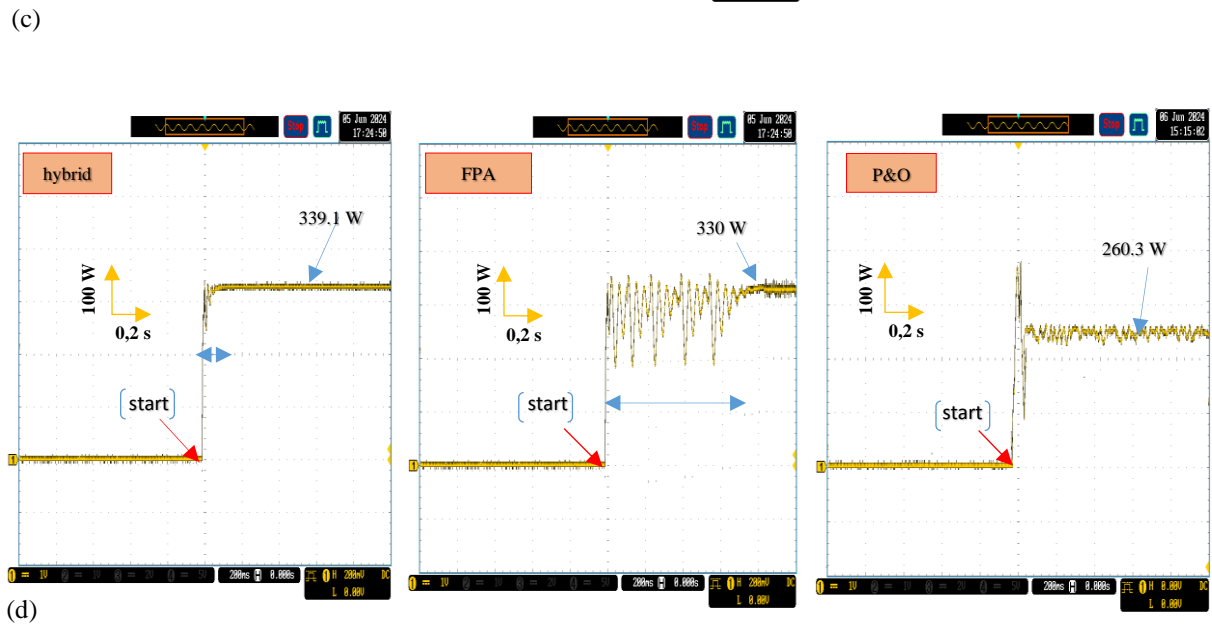
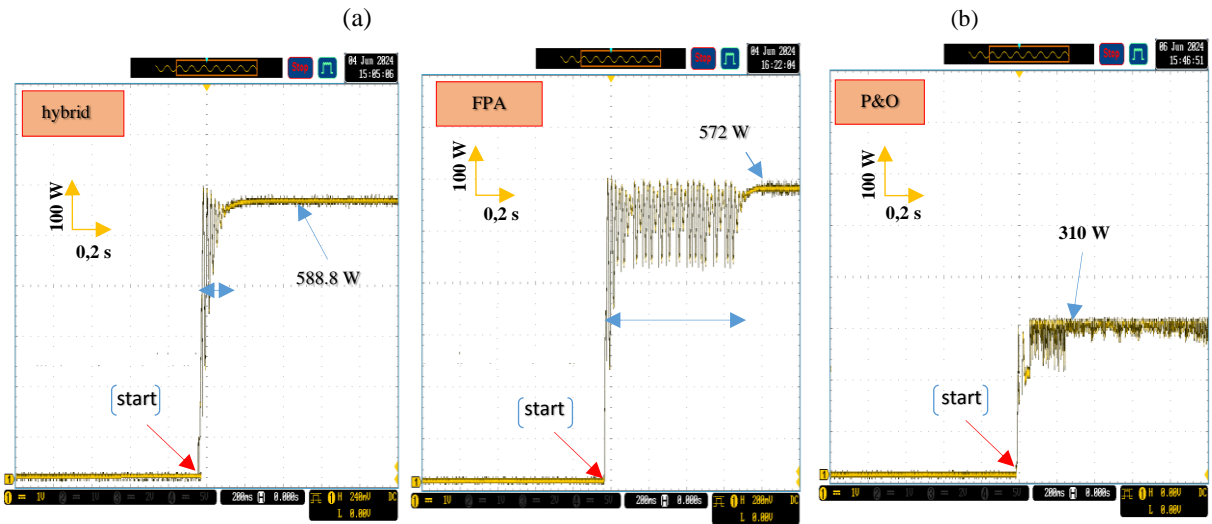
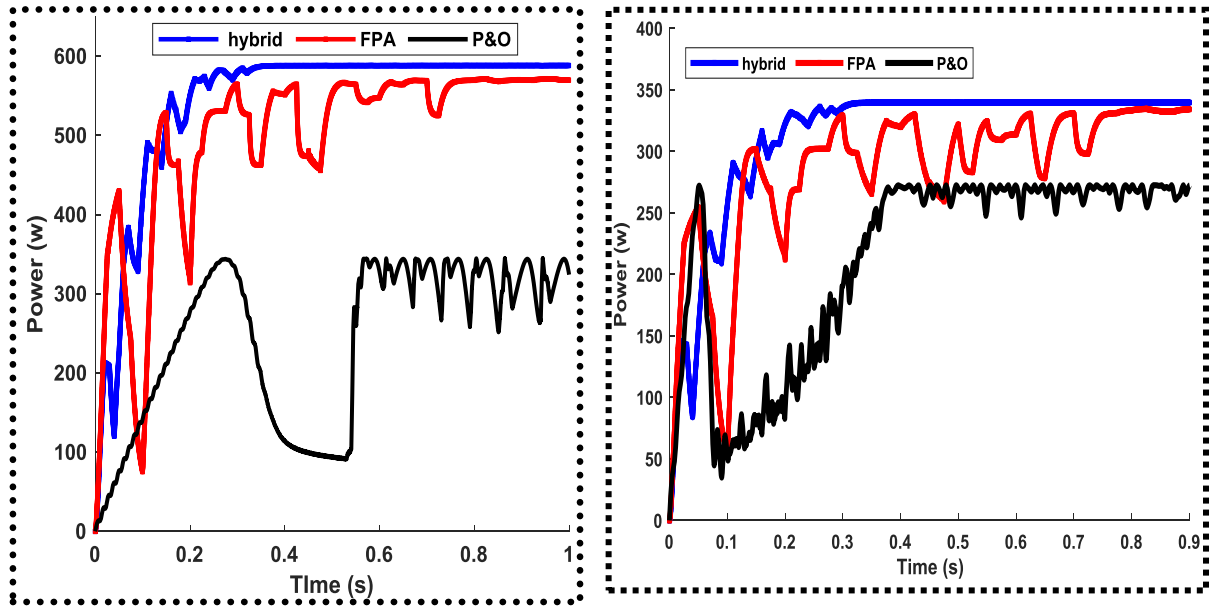
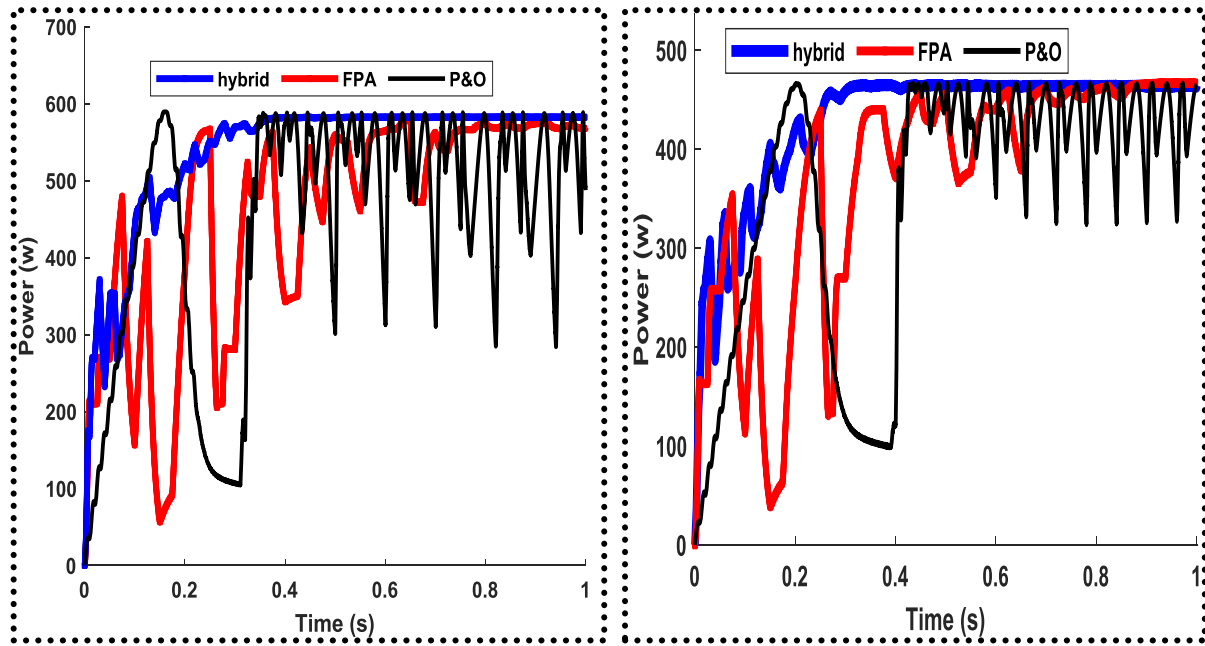
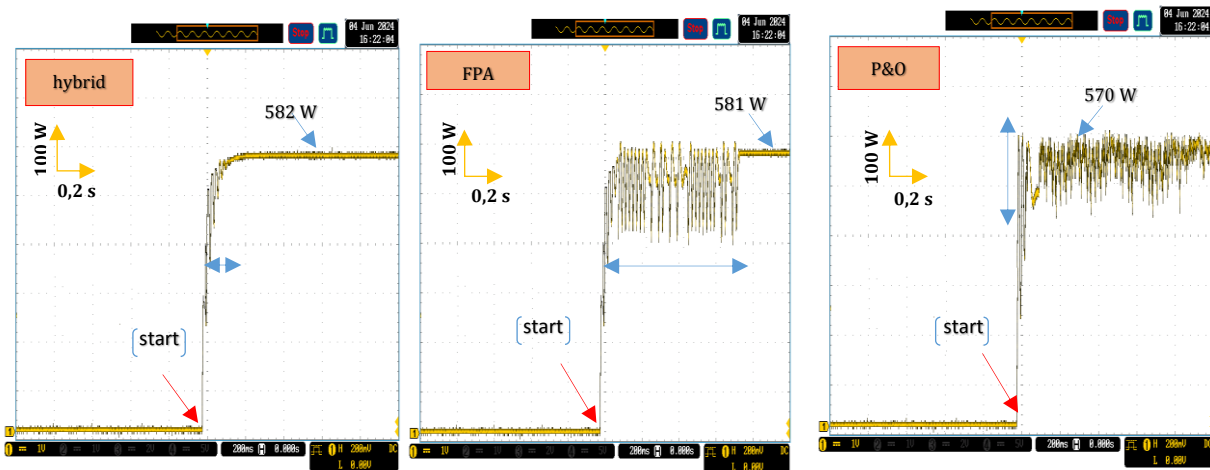


Fig 6. Tracking Process of GMPP in Simulation and HIL Experimental Results of Pattern 1 and Pattern 2.

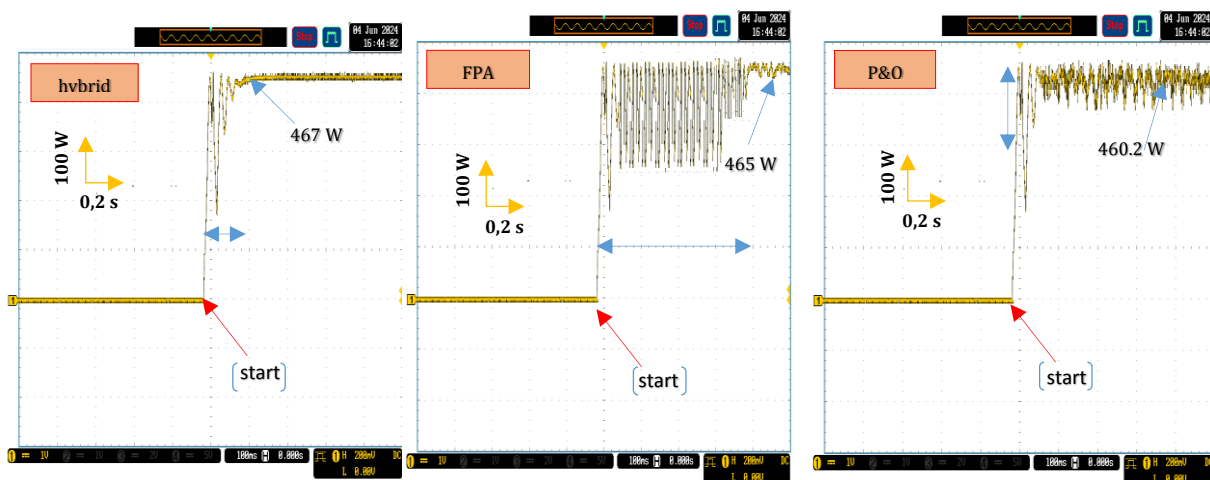


(a)

(b)



(c)



(d)

Fig 7. Tracking Process of GMPP in Simulation and HIL Experimental Results of Pattern 2 and Pattern 3.

Fig. 8 shows that the hybrid algorithm achieved the lowest RMSE, RME and RE when compared to the FPA and P&O algorithms. This shows that the hybrid algorithm more accurately follows the GMMP with minimal oscillations. Moreover, this also features the fastest convergence and the stability of GMPPs.

The results the effectiveness of the P&O-FPA algorithm as shown in Figure 9, which combines the strengths of both P&O and FPA. This hybrid approach, takes advantage of speed the P&O algorithm's speed in tracking changes in the power output and from FPA's capability to accurately identify the Global Maximum Power Point (GMPP).

As a result, the P&O-FPA algorithm has proven to be a successful and promising solution, delivering excellent performance in optimizing photovoltaic systems under varying shading patterns and conditions. This combination of speed and precision makes it a valuable choice for maximizing power output in practical applications.

A performance comparison of the proposed control method and other methods used for the same characteristic is summarized in Table 1. This comparison is based on the maximum power output (P_{max}), the accuracy (%) of each control system, convergence time, and optimal duty cycle. The proposed hybrid MPPT demonstrates superior performance across all metrics.

Fig. 10 shows boxplots comparing the accuracy and convergence time of different MPPT algorithms. The proposed hybrid FPA–P&O method achieves the highest accuracy and fastest convergence with minimal variation, confirming its superior performance under partial shading conditions.

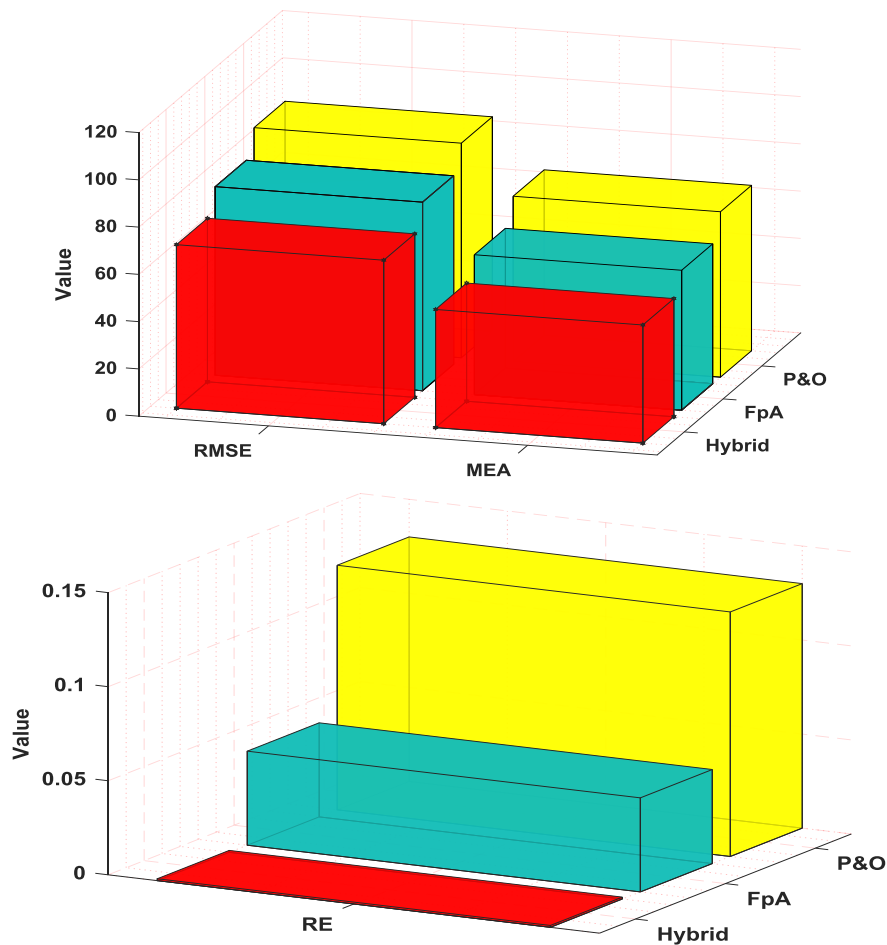


Fig 8. Comparison of RMSE, MAE and RE.

Table 1. Comparison between the Proposed technique and other methods.

Shading Pattern	Pmax (W)					Accuracy (%)			
	Target	PSO	GWO	HOA	Hybrid Proposed	PSO	GWO	HOA	Hybrid Proposed
Pattern 1	588.8	569.6	572.02	588.5	588.7	96.73	97.15	99.94	99.99
Pattern 2	339.9	320.3	330	339.1	339.8	94.2	97.08	99.76	99.99
Pattern 3	582.2	561.5	571.3	581.4	582.1	96.27	98.12	99.86	99.99
Pattern 4	467.1	461.2	464	467.05	467.08	98.73	99.33	99.98	99.99

Shading Pattern	Convergence (second)				Optimal duty cycle			
	PSO	GWO	HOA	Hybrid Proposed	PSO	GWO	HOA	Hybrid Proposed
Pattern 1	0.76	0.32	0.31	0.25	0.615	0.601	0.609	0.607
Pattern 2	0.78	0.33	0.32	0.28	0.490	0.452	0.468	0.462
Pattern 3	0.89	0.36	0.35	0.29	0.695	0.680	0.685	0.683
Pattern 4	0.85	0.31	0.29	0.27	0.527	0.548	0.530	0.528

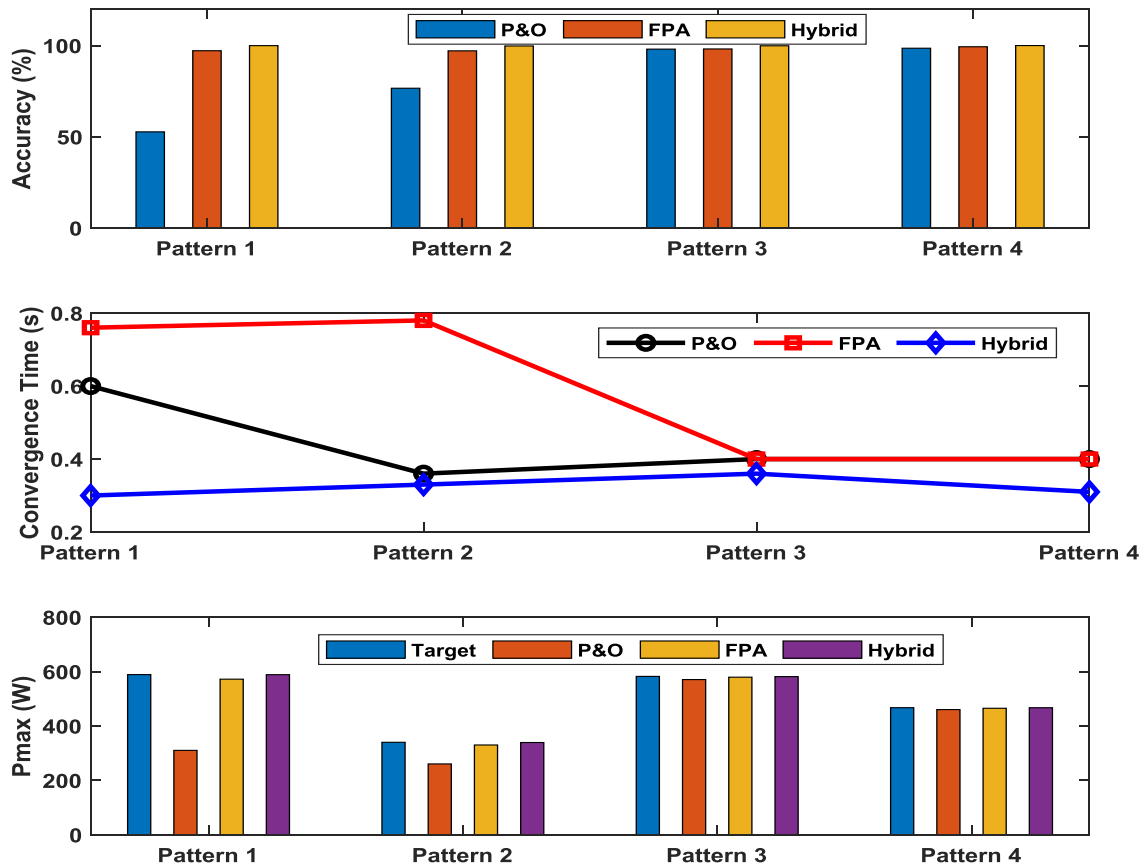


Fig 9. Quantitative comparison between MPPT.

MPPT board's cost analysis

The cost of hardware used for implementing MPPT algorithms plays a critical role in determining the feasibility and scalability of photovoltaic (PV) systems, particularly for deployment in cost-sensitive environments. Many advanced MPPT strategies rely on high-end platforms such as OPAL-RT, Typhoon HIL, or MicrolabBox, which, while offering robust real-time performance and precise control, come at a substantial financial cost often exceeding \$20,000. In contrast, the present study employs two dSPACE

DS1104 boards, with an estimated project-level allocation cost of \$1,500–\$2,000. Despite this significantly lower investment, the proposed hybrid FPA–P&O algorithm achieves competitive performance, validated through hardware-in-the-loop (HIL) experiments under dynamic partial shading conditions. This demonstrates a superior cost-to-performance ratio compared to several recent works, as shown in Table 2.

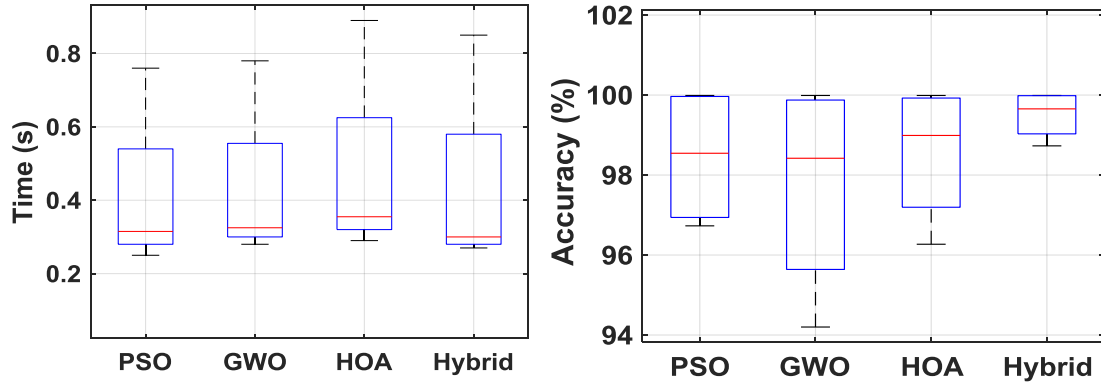


Fig 10. Boxplot for qualitative performance comparison between MPPT algorithms.

Table 2. Comparative Analysis of MPPT Implementations

Study / Approach	MPPT Method	Platform / Environment	Approx. Cost (USD)	Performance Validation
Al-Shammaa et al. (2022)	Cuckoo Search Optimization (CSO)	OPAL-RT OP4510 + dSPACE 1104	\$30,000	HIL; GMPP tracked in 0.99–1.32 s; CSO outperforms PSO in PSC conditions.
Rehman et al. (2023)	Driving Training-Based Optimization (DTBO)	Typhoon 402	\$25,000–\$30,000	Real-time HIL. validated against PSO, JAYA, and AJAYA under PSCs; fast and stable tracking.
Al-Hussein et al. (2025)	Synergetic Control Theory (SCT)	FPGA-based digital controller	\$5,000–\$10,000	Fixed-point FPGA MPPT controller; robust under irradiance/temp changes; smooth and precise MPPT response.
Abo-Khalil et al. (2023)	Simulated Annealing- (SA-P&O)	MicrolabBox + DC-DC/AC converters + L filter	\$20,000	Real converter setup; SA improves convergence of classical P&O under shading; validated under dynamic and static conditions.
González-Castaño et al. (2021)	Support Vector Machine (SVM)	PLECS RT Box 1 + TI LAUNCHXL-F28069M	\$12,000–\$15,000	HIL validated MPPT controller with reduced steady-state oscillations; tested under varying irradiance and temperature.
Fu et al. (2022)	Improved Slime Mold Algorithm	HIL + Rapid Control Prototyping (Yuankuan platform)	\$10,000	Tested against PSO, SSA, TSO, BWO; fastest convergence, fewest power fluctuations; verified on FPGA-CPU RCP platform.
Bo Yang et al. (2019)	Atom Search Optimization (FASO)	Two dSPACE DS1104 + dSPACE DS1006	\$20,000	Validated on TEG system; GMPP tracking accuracy >98%, <2.3% difference between simulation and HIL results.

Table 2. Comparative Analysis of MPPT Implementations (*Continued*)

Study / Approach	MPPT Method	Platform / Environment	Approx. Cost (USD)	Performance Validation
Saibal Manna et al. (2023)	Lyapunov-based Adaptive Control (LRMRAC)	OPAL-RT OP4510 simulator	\$30,000	HIL-tested under abrupt/shaded conditions; GMPP tracked in <10 ms; outperforms ANFIS, INC, VSPO, and P&O.
Jia Shun Koh et al. (2024)	Deterministic Peak Hopping (PH)	TI C2000 MCU + ITECH IT6012C-800-40 PV simulator	>\$2,000	Simple PH mechanism handles >5 close peaks; tracking accuracy >98.7%; implemented in real-time with fast convergence.
This Work	Hybrid FPA-P&O	Two dSPACE DS1104 boards	\$1,500-\$2,000	HIL implementation under PSC; 99% tracking efficiency; nearly zero GMPP oscillation; superior performance vs. classical P&O and FPA.

6. CONCLUSION

In conclusion, this paper has investigated the performance of a hybrid Flower Pollination Algorithm–Perturb and Observe (FPA-P&O) Maximum Power Point Tracking (MPPT) technique through Hardware-in-the-Loop (HIL) testing, aiming to optimize photovoltaic (PV) systems under partial shading conditions. The results demonstrated the superior effectiveness of the hybrid P&O-FPA method over its standalone counterparts. Notably, the hybrid approach achieved higher power extraction and exhibited significantly reduced steady-state oscillations, ensuring more reliable performance across all shading scenarios. In contrast, individual algorithms such as FPA and P&O struggled with energy and time inefficiencies, often failing to identify the global maximum power point (GMPP) consistently. These limitations underscore the advantages of the hybrid technique in enhancing MPPT robustness and efficiency under real-world shading complexities.

REFERENCES

- Abo-Khalil, A. G., El-Sharkawy, I. I., Radwan, A. and Memon, S. (2023). Influence of a Hybrid MPPT Technique, SA-P&O, on PV System Performance under Partial Shading Conditions, *Energies*, 16(2), 577, doi: 10.3390/en16020577.
- Al-Hussein, A.-B. A., Tahir, F. R. and Pham, V.-T. (2025). FPGA Implementation of Synergetic Controller-Based MPPT Algorithm for a Standalone PV System, *Computation*, 13(3), 64, doi: 10.3390/computation13030064.
- Al-Shammaa, A.A., Abdurraqeeb, A.M., Noman, A.M., Alkuhayli, A. and Farh, H.M.H. (2022). Hardware-In-the-Loop Validation of Direct MPPT Based Cuckoo Search Optimization for Partially Shaded Photovoltaic System, *Electronics*, 11(10), 1655. doi: 10.3390/electronics11101655.
- Baba, A.O., Liu, G. and Chen, X. (2020). Classification and Evaluation Review of Maximum Power Point Tracking Methods, *Sustainable Futures*, 2.
- Bayrak, F., Ertürk, G. and Oztop, H.F. (2017). Effects of partial shading on energy and exergy efficiencies for photovoltaic panels, *Journal of Cleaner Production*, 164, 58–69, doi: 10.1016/j.jclepro.2017.06.108.

- Bettahar, F., Sabrina, A. and Achour, B. (2023). Enhancing PV Systems with Intelligent MPPT and Improved control strategy of Z-Source Inverter, *Power Electronics and Drives*, 9(1), 1–20, doi: 10.2478/pead-2024-0001.
- Bhukya, M. N. and Kota, V. R. (2018). A novel P&OT-Neville's interpolation MPPT scheme for maximum PV system energy extraction, *International Journal of Renewable Energy Development*, 7(3), 251–260, doi: 10.14710/ijred.7.3.251-260.
- Bollipo, R.B., Mikkili, S. and Bonthagorla, P.K. (2020). Critical Review on PV MPPT Techniques: Classical, Intelligent and Optimisation, *IET Renewable Power Generation*, 14, 1433–1452, doi: 10.1049/iet-rpg.2019.1163.
- Chai, L.G.K., Gopal, L., Juwono, F.H., Chiong, C.W.R., Ling, H.-C. and Basuki, T.A. (2021). A novel global MPPT technique using improved PS-FW algorithm for PV system under partial shading conditions, *Energy Conversion and Management*, 246, 114639, doi: 10.1016/j.enconman.2021.114639.
- Chauhan, U., Rani, A., Kumar, B. and Singh, V. (2019). A multi verse optimization based MPPT controller for drift avoidance in solar system, *Intelligent & Fuzzy Systems*, 36, 2175–2184.
- Chellal, M., Guimarães, T.F. and Leite, V. (2021). Experimental Evaluation of MPPT algorithms: A Comparative Study, *International Journal of Renewable Energy Research*, 11(1), doi: 10.20508/ijrer.v11i1.11797.g8164.
- Fares, B., Sabrina, A. and Achour, B. (2024). A Comparative Study of PSO, GWO, and HOA Algorithms for Maximum Power Point Tracking in Partially Shaded Photovoltaic Systems, *Power Electronics and Drives*, vol. 9(44), doi: 10.2478/pead-2024-0006.
- Fares, B., Sabrina, A., Achour, A. and Omar, C. (2023). Power quality improvement by using photovoltaic based PSO as MPPT with Space vector modulation (SVM) control strategy of Quasi Z-Source inverter, in *2023 1st Int. Conf. on Renewable Solutions for Ecosystems: Towards a Sustainable Energy Transition (ICRSEtoSET)*, doi: 10.1109/ICRSEtoSET56772.2023.10525472.
- Fares, B., Sabrina, A., Achour, B. Ishak, K, Short, M.M., Al-Greer. (2025). Experimental Optimization of Photovoltaic System Performance Using an Enhanced Flower Pollination Algorithm under Partial Shading Conditions. In *NC-REAEE'25: The First National Conference on Renewable Energies and Advanced Electrical Engineering*, Msila, Algeria, May 6–7.
- Fekkak, B., Mena, M., Boussahoua, B. and Rekioua, D. (2019). Processor in the loop test for algorithms designed to control power electronics converters used in grid-connected photovoltaic system, *International Transactions on Electrical Energy Systems*, doi: 10.1002/2050-7038.12227.
- Fu, C., Zhang, L., and Dong, W. (2022). Research and Application of MPPT Control Strategy Based on Improved Slime Mold Algorithm in Shaded Conditions, *Electronics*, 11(14), 2122, doi: 10.3390/electronics11142122.
- González-Castaño, C., Marulanda, J., Restrepo, C., Kouro, S., Alzate, A. and Rodriguez, J. (2021). Hardware-in-the-Loop to Test an MPPT Technique of Solar Photovoltaic System: A Support Vector Machine Approach, *Sustainability*, 13(6), 3000, doi: 10.3390/su13063000.
- Koh, J. S., Tan, R. H. G., Lim, W. H. and Tan, N. M. L. (2024). A Real-Time Deterministic Peak Hopping Maximum Power Point Tracking Algorithm for Complex Partial Shading Condition, *IEEE Access*, 12, 43632–43644, doi: 10.1109/access.2024.3380844.
- Krishna, K. S. and Kumar, K.S. (2015). A review on hybrid energy systems, *Renewable and Sustainable Energy Reviews*, 52, 907–916, doi: 10.1016/j.rser.2015.07.187.

- Mai, C., Zhang, L. and Hu, X. (2024). Combining dynamic adaptive snake algorithm with perturbation and observation for MPPT in PV systems under shading conditions, *Applied Soft Computing*, 162, 111822, doi: 10.1016/j.asoc.2024.111822.
- Manna, S., Akella, A.K. and Singh, D.K. (2023). Novel Lyapunov-based rapid and ripple-free MPPT using a robust model reference adaptive controller for solar PV system, *Protection and Control of Modern Power Systems*, 8(1), doi: 10.1186/s41601-023-00288-9.
- Mohanty, S., Subudhi, B., and Ray, P.K. (2017). A Grey Wolf-Assisted Perturb & Observe MPPT Algorithm for a PV System, *IEEE Transactions on Energy Conversion*, 32(1), 340–347, doi: 10.1109/tec.2016.2633722.
- Nassef, A.M., Abdelkareem, M.A., Maghrabie, H.M. and Baroutaji, A. (2023). Review of Metaheuristic Optimization Algorithms for Power Systems Problems, *Sustainability*, 15(12), 9434, 2023, doi: 10.3390/su15129434.
- Rehman, H. et al. (2023). Driving training-based optimization (DTBO) for global maximum power point tracking for a photovoltaic system under partial shading condition, *IET Renewable Power Generation*, 17(10), 2542–2562, doi: 10.1049/rpg2.12768.
- Samano-Ortega, V., Padilla-Medina, A., Bravo-Sanchez, M., Rodriguez-Segura, E., Jimenez-Garibay, A. and Martinez-Nolasco, J. (2020). Hardware in the Loop Platform for Testing Photovoltaic System Control, *Applied Sciences*, 10(23), 8690, doi: 10.3390/app10238690.
- Senapati, Ma., Senapati, Mr. and Panigrahi, P. (2023). Efficient Maximum Power Point Tracking Algorithm for Photovoltaic Systems under Partial Shading Conditions: Hybrid FSSO-HHO Approach with Hardware-in-Loop Validation, doi: 10.21203/rs.3.rs-2983874/v1.
- Yang B. et al., (2020). Fast atom search optimization based MPPT design of centralized thermoelectric generation system under heterogeneous temperature difference, *Journal of Cleaner Production*, 248, 119301, doi: 10.1016/j.jclepro.2019.119301.
- Yang, Y. and Wen, H. (2018). Adaptive perturb and observe maximum power point tracking with current predictive and decoupled power control for grid-connected photovoltaic inverters, *Journal of Modern Power Systems and Clean Energy*, 7, 422–432, doi: 10.1007/s40565-018-0437-x.
- Zhao, A., Wu, W., Sun, Z., Zhu, L., Lu, K., Chung, H.S. and Blaabjerg, F. (2019). A Flower Pollination Method Based Global Maximum Power Point Tracking Strategy for Point-Absorbing Type Wave Energy Converters, *Energies*, 12(7), 1343, doi: 10.3390/en12071343.